Bilateral Motion Spectra
Analysis and Representation of Human Movement

Anthony Schultz[1]
[1]*Department of Science and Dance, Sarah Lawrence College, One Mead Way, Bronxville NY, USA*
aschultz@slc.edu

Keywords: Motion Capture Analysis, Pattern Recognition, Human Movement, Data Representation.

Abstract: The body's bilateral symmetry allows for various kinds of human motion patterns. Our paper presents a method for analyzing and representing motion capture time series that effectively identifies spatial and temporal patterns. We develop a factored representation of joint angle data based on quaternions and a metric pair for comparing different physical states of articulation. This metric pair is used to generate a metric space pair over the set of time series states. The result is represented as a 2-dimensional color image termed a bilateral motion spectrum. Several spectral motifs are presented and characterized.

1 INTRODUCTION

Motion capture is a standard form of acquiring kinematic data from human subjects using an animated stick-figure model. Systems are available at a range of price points from the consumer grade Kinect to more elaborate multi-camera marker systems such as those made by VICON. All motion capture systems provide skeletal model joint angles in time series. The informational content of such high dimensional datasets are challenging to represent in a concise and meaningful way.

There has been extensive research in motion capture data processing. One such area of research processes motion capture datasets with the goal of remixing recorded libraries to generate novel movement sequences. A data structure known as a motion graph is generated to determines how elements of given a movement vocabulary may be sequenced in time. In these research efforts recognition schemes are used to compare frames of motion capture data to see where different phrases of movement may be spliced together. If two frames match we can conceivably cut from one sequence of motion to another thereby generating a novel movement sequence.

Mathematically speaking the similarity measure between frames is termed a metric. It is a measure of distance between two points in the configuration space of the subject's body. Analyzing a motion sequence by comparing the similarity between each frame and every other frame is a common process. The output of this process is a metric space. Due to its features we call this output a motion spectrum.

While motion spectra are typically a means to an end, namely a way to construct the subject's motion graph, they are full of information about temporal features of the underlying movement. Motion spectra convey the rapidity of movement, when motions are repeated and when they are executed in reverse. Our review of the literature indicates there has not been any research into characterizing human movements by investigating their associated motion spectra.

This paper seeks to introduce such a line of research. By enhancing motion spectra to include measurements on the spatial and temporal symmetries of motion capture sequences we generate a richer data structure we call a bilateral motion spectrum. In this paper we detail how to construct bilateral motion spectra, process example motion capture data and characterize the resulting spectral motifs.

1.1 Motion Capture Data

Motion capture models the human body as set of rigid element joined at points of articulation, or joints. This model is known as a kinematic chain. The articulation of each joint, represented by joint angles, uniquely determines the state of kinematic model.

This work uses optical motion capture data which is publicly available online from the Carnegie Mellon Motion Capture Lab in the ASF/AMC format. The kinematic chain model they use has a total of 62 degrees of freedom. The ASF data (Acclaim Skeleton File) describes the geometry of the kinematic chain.

This includes the segment lengths and their linkage hierarchy. The AMC data (Acclaim Motion Capture) consists of the joint angles and the root coordinate system position. Joint angles are reported by Euler angle in XYZ order of rotation.

In the present treatment we use a simplified version of the ASF model. We model the axial skeleton with seven links. They are the pelvis (root), lowerback, upperback, thorax, lowerneck, upperneck and head. Each joint connecting these links is spherical with three degrees of freedom. Off the pelvis we have the left and right leg. Each is modeled with two links, the femur and tibia. The femur having a spherical joint (3 DOF) and the tibia having a revolute joint (1 DOF). The left and right arm are measured in the same way as the legs. They branch off the thorax link of the axial skeleton with the humerus having a spherical joint (3 DOF) and the radius having a revolute joint (1 DOF).

1.2 Related Work

Using metric spaces of example movement data to construct motion graphs is over a decade old. This process was developed by (Arikan and Forsyth, 2002) and (Kovar et al., 2002) and detailed by (Alankus, 2005) in a comprehensive thesis. The challenge in building a motion graph is knowing where to splice the motion capture threads together. There are various metrics used for this purpose. Some are based solely on joint angle which others are based on point clusters. While some are more sophisticated than others none use the metric spaces to characterize the motion itself.

2 MATHEMATICS

2.1 Rotations

ASF data represents joint angle rotations using Euler angles in XYZ order of rotation. The successive rotations may be used to construct the overall rotation matrix using matrix multiplication.

$$R_{zyx}(\theta_x,\theta_y,\theta_z) = R_z(\theta_z)R_y(\theta_y)R_x(\theta_x)$$

This method suffers from gimbal lock so it requires reparameterization for our purposes. The rotation matrix may be expressed as a single rotation θ around the Euler pole vector $\vec{\omega}$ using Equations 1 and 2. (Murray et al., 1994)

$$\theta = \cos^{-1}\left(\frac{trace(R)-1}{2}\right) \tag{1}$$

$$\vec{\omega} = \frac{1}{2\sin\theta}\begin{pmatrix} r_{32}-r_{23} \\ r_{13}-r_{31} \\ r_{21}-r_{12}\end{pmatrix} \tag{2}$$

Using the terms θ and $\vec{\omega}$ we can switch from matrices to a more compact representation using quaternions. Quaternions are a 4-tuple consisting of a real component q_0 and three imaginary components $q_1 i + q_2 j + q_3 k$. The algebra of the imaginary components follows is written in Equation 3.

$$ii = jj = kk = ijk = -1 \tag{3}$$

The imaginary components may be written as a vector $\vec{q}$ so that the overall quaternion Q may be written as in Equation 4.

$$Q = \begin{pmatrix} q_0 \\ \vec{q}\end{pmatrix} \tag{4}$$

Quaternions may be be used to represent rotations using the Euler axis formalism as in Equation 5. (Murray et al., 1994)

$$\begin{pmatrix} q_0 \\ \vec{q}\end{pmatrix} = \begin{pmatrix} \cos(\theta/2) \\ \sin(\theta/2)\vec{\omega}\end{pmatrix} \tag{5}$$

2.2 Configuration Space

We collect the set of quaternions determining the pose of the body model into a state or configuration vector $\vec{\Psi}$. We begin with a basis in which each element of the vector, quaternion Q_i, determines the rotational state of joint i. The quaternions, which represent a set of rotational transformations, constitute a manifold. This manifold is called the configuration space, or $\mathcal{C}$, of the kinematic chain. The state vector $\vec{\Psi}$ spans $\mathcal{C}$.

In other words, each physical configuration of the kinematic chain model is associated with a state vector $\vec{\Psi}$. In turn, this configuration vector (state vector) is associated with a point in the configuration space $\mathcal{C}$. These three representations are shown in Figure 1.

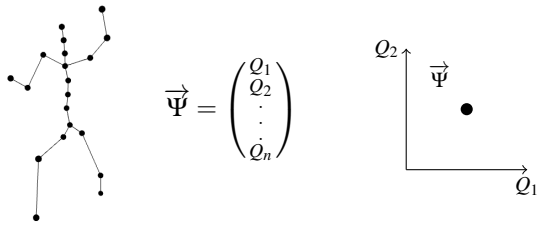

Figure 1: Three equivalent representations of a kinematic state.

2.3 Distance Metric

In order to compare two configuration states, $\vec{\Psi}_a$ and $\vec{\Psi}_b$, we define a distance function or metric. We begin by using a metric to compare each rigid element

separately and then combine these distance functions to generate a distance metric comparing whole states of the whole body. A distance metric measuring the difference between two poses is depicted in Figure 2.

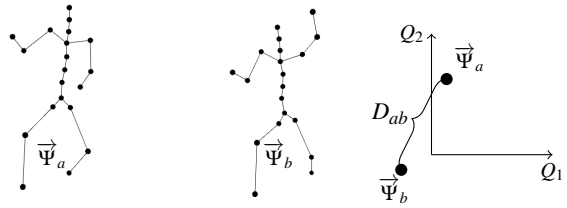

Figure 2: Distance measure between two states in $\mathcal{C}$

We follow the usual definition for metrics as a map $D : \mathcal{C} \times \mathcal{C} \rightarrow \mathbb{R}$ satisfying the following four axioms: non-negativity stated in Equation 6, indiscernability stated in Equation 7, symmetry stated in Equation 8 and subadditivity stated in Equation 9. (Huynh, 2009)

$$D(x,y) \geq 0 \tag{6}$$

$$D(x,y) = 0 \Leftrightarrow x = y \tag{7}$$

$$D(x,y) = D(y,x) \text{ for } x,y \in \mathcal{C} \tag{8}$$

$$D(x,z) \leq D(x,y) + D(y,z) \text{ for } x,y \in \mathcal{C} \tag{9}$$

We use the inner product of quaternions as our metric for comparing the rotational states of rigid elements. We define the inner product operator for quaternions in Equation 10as a 4-tuple dot product. (Huynh, 2009)

$$Q \circ G = q_0 g_0 + q_1 g_1 + q_2 g_2 + q_3 g_3 \tag{10}$$

In Equation 11 we use the inner product of quaternions to derive a distance metric based solely on the rotational state of a particular rigid body element.

$$D(Q_a, Q_b) = 1 - Q_a \circ Q_b \tag{11}$$

This metric is a measure in SO(3) and gives values in the range [0,1].

Equation 12 constructs a metric between whole body configurations using weighted sum of metrics for individual links.

$$D(\overrightarrow{\Psi}_a, \overrightarrow{\Psi}_b) = \Sigma_i w_i D(Q_{ai}, Q_{bi}) \tag{12}$$

This whole body metric gives values in the range $[0,\Sigma_i w_i]$. It measures the difference between two different states of the body $\overrightarrow{\Psi}_a$ and $\overrightarrow{\Psi}_b$. The states are normalized so that the whole body metric has the form shown in Equation 13.

$$D_{ab} = 1 - \overrightarrow{\Psi}_a \circ \overrightarrow{\Psi}_b \tag{13}$$

2.4 Metric Spaces and Similarity Matrices

We notate each motion path as a set of states over a time index, $\overrightarrow{\Psi}(t_i)$ and create a metric space D_{ij} over this set by calculating the distance between each element of the set using the double index ij.

$$D_{ij} = D(\overrightarrow{\Psi}(t_i), \overrightarrow{\Psi}(t_j)) \tag{14}$$

Using the elements of D_{ij} we create a 2D array called the similarity matrix, Z_{ij}. The indiscernability property of D, stated in Equation 7, requires all diagonal elements of the matrix Z_{ij} are equal to one while the symmetry property of D, stated in Equation 8, requires the matrix Z_{ij} is symmetric.

$$Z_{ii} = 1 \tag{15}$$

$$Z_{ij} = Z_{ji} \tag{16}$$

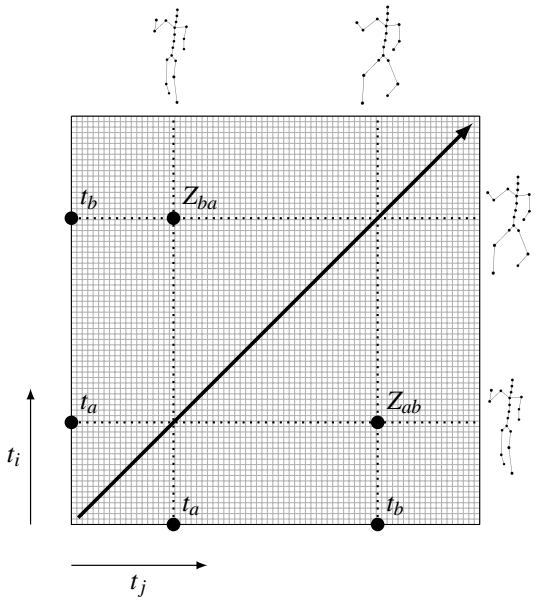

Figure 3: Similarity matrix Z_{ij}.

3 Motion Spectra

Mapping Z_{ij} matrix element values to greyscale values produces an image which conveys motion path information visually as shown in Figure 4. Z_{ij} values of 0 are mapped to black, 0 in the greyscale. Values of 1 are mapped to white, 256 in the greyscale. All Z_{ij} values between 0 and 1 are mapped to the greyscale linearly. The intensity of the Z_{ij} matrix element determines the similarity between $\overrightarrow{\Psi}(t_i)$ and $\overrightarrow{\Psi}(t_j)$. We

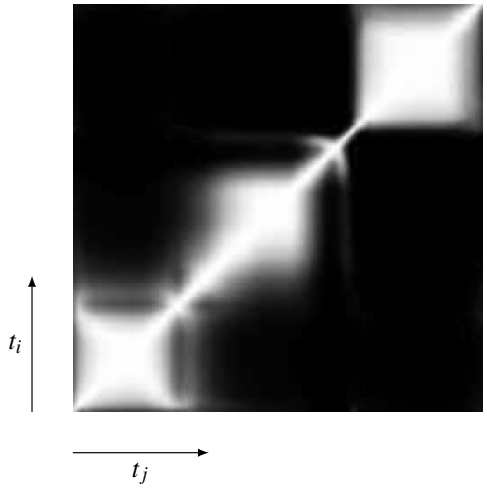

Figure 4: A motion spectrum is the the similarity matrix Z_{ij} represented in greyscale.

call these images motion spectra. We term the light regions within them proximity signals.

We call the diagonal elements of the similarity matrix Z_{ij} the identity axis since these are equal to one, as they are in the standard identity matrix. The elements near the identity axis are of interest because they give us insight into how the configuration state $\overrightarrow{\Psi}(t)$ changes over time.

Since Z_{ij} is a symmetric matrix we can represent it more compactly as a the upper left triangular portion rotated 45 degrees so that the identity axis is horizontal. This horizontal axis is used as a $t_{i=j}$ time axis. From this view time runs horizontally to the right and similarity between states at various times is indicated by elements of the triangle.

3.1 Rapidity and Stillness

There are identifiable visual features of motion spectra near the identity axis relating to the rapidity of movement. Equation 17 defines rapidity as magnitude of the time rate of change of the configuration state and gives a way to find its measure using the distance metric.

$$|\frac{d\overrightarrow{\Psi}(t)}{dt}| = \frac{D(\overrightarrow{\Psi}(t_i), \overrightarrow{\Psi}(t_{i-1}))}{\Delta t} \qquad (17)$$

The wider the proximity signal along the identity axis the less displacement there is over time. This means the subject is slow moving. Said another way, the thinner proximity signal along the identity axis the more rapidly the subject is moving. Figure 5 shows the rotated triangular version of the motion spectrum Figure 4.

Below the identity axis we show corresponding images of the kinematic chain model where at each time point we overlap models for states $\overrightarrow{\Psi}(t)$ and $\overrightarrow{\Psi}(t+\Delta)$. In this instance the Δ is 20 frames or a sixth of a second. It sections of the motion path with more displacement correspond to thinner width of the identity axis.

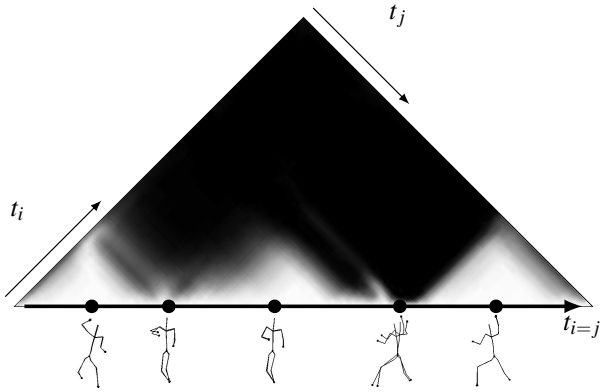

Figure 5: Kinematic displacement is related to the width Z_{ij} signal in the neighborhood of the identity axis.

The lack of displacement of the kinematic model over time can be interpreted as stillness. Though the model may not actually be still the kinematic states all reside within a certain region of $\mathcal{C}$ in which all points are within a certain proximity to one another. Continued presence in this region over time is described as stillness. This is visible in Figure 5.

3.2 Repetition

3.2.1 State Repetition

Figure 6 shows a spectrum in which a begins and ends in the same state in $\mathcal{C}$. The off diagonal region of lightness is a proximity signal indicating a similarity between $\Psi(t_a)$ and $\Psi(t_b)$. The return of a motion path to a previously inhabited region of $\mathcal{C}$ manifests an off diagonal proximity signal in Z_{ij} indicating proximity between $\Psi(t_a)$ and $\Psi(t_b)$ in $\mathcal{C}$.

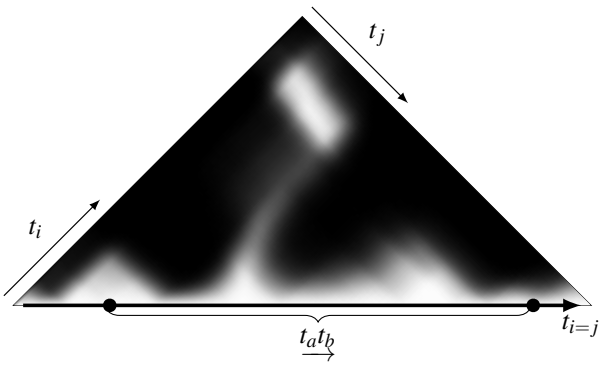

Figure 6: Example of state repetition.

3.2.2 Path Repetition

Figure 7 shows a spectrum in which two motion paths travel along the same route in $\mathcal{C}$. The off diagonal horizontal light region indicates a similarity between $\Psi(\underrightarrow{t_a t_b})$ and $\Psi(\underrightarrow{t_c t_d})$. An off diagonal signal which looks like the identity axis signal is a visual motif indicating repetition of movement.

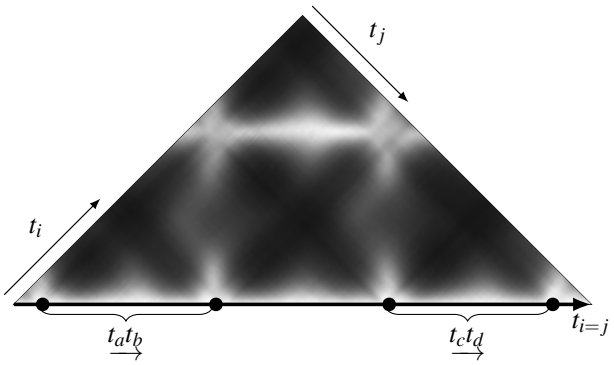

Figure 7: Example of motion path repetition.

3.2.3 Palindromic Repetition

Figure 8 shows a spectrum in which two motion paths travel along the same route in $\mathcal{C}$ but in opposite directions. This type of motion, when a movement is executed and then repeated backwards in time, is termed palindromic. A proximity signal projecting perpendicularly from the identity axis indicates a similarity between $\Psi(\underrightarrow{t_a t_b})$ and the time reversed version of $\Psi(\underrightarrow{t_b t_c})$.

$$\Psi(\underrightarrow{t_a t_b}) = \Psi(\underleftarrow{t_b t_c}) \tag{18}$$

We notate this time reversal using a left under arrow. An off diagonal signal which looks like the identity axis signal but projected perpendicular to it is the visual motif palindromic repetition.

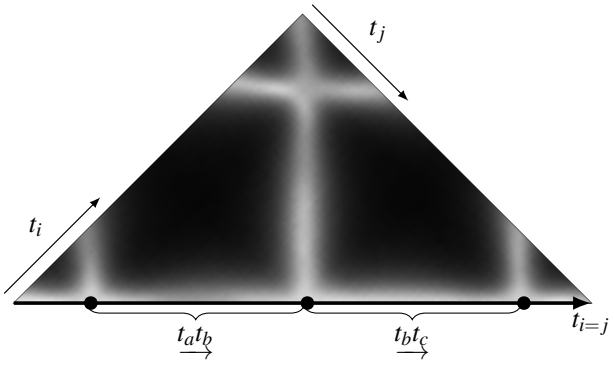

Figure 8: Example of palindromic path repetition.

4 BILATERAL SPECTRA

4.1 Reflection

Due to the symmetry of the human body we know for any configuration state $\overrightarrow{\Psi} \in \mathcal{C}$ there exists a mirror image configuration state $\overrightarrow{\Psi}^* \in \mathcal{C}$. The reflection transformation maps the state of the body from $\overrightarrow{\Psi} \rightarrow \overrightarrow{\Psi}^*$. We represent the reflection transformation in Figure 9.

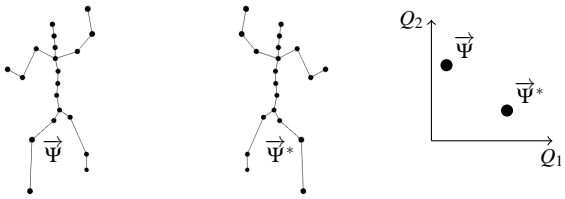

Figure 9: Reflected pose and corresponding points in $\mathcal{C}$.

4.1.1 Reflection Pseudometric

A pseudometric follows non-negativity and symmetry but lacks the indiscernability of proper metrics. Equation 19 defines the reflection pseudometric D^*_{ab}. This is the metric distance between state $\overrightarrow{\Psi}_a$ and the reflection of state $\overrightarrow{\Psi}_b$.

$$D^*_{ab} = 1 - \overrightarrow{\Psi}_a \circ \overrightarrow{\Psi}^*_b \tag{19}$$

We define the metric pair as the set of values D_{ab} and D^*_{ab}.

4.2 Anti-Similarity Matrices and Spectra

We construct the anti-similarity matrix Z^*_{ij} and anti-similarity spectrum as we did in the previous section. Equation 20 defines a pseudometric space by calculating the reflection pseudometric between each element of the set using the double index ij.

$$D^*_{ij} = D^*(\overrightarrow{\Psi}(t_i), \overrightarrow{\Psi}(t_j)) \tag{20}$$

Using this matrix of distance values we create a 2D array for Z^*_{ij} termed the anti-similarity matrix. Figure 10 shows an example. The corresponding image form of the matrix, which maps matrix elements to greyscale pixel values, is referred to as the anti-similarity spectrum.

The symmetry property of the pseudometric space D^*_{ij} requires Z^*_{ij} is symmetric.

$$Z^*_{ij} = Z^*_{ji} \tag{21}$$

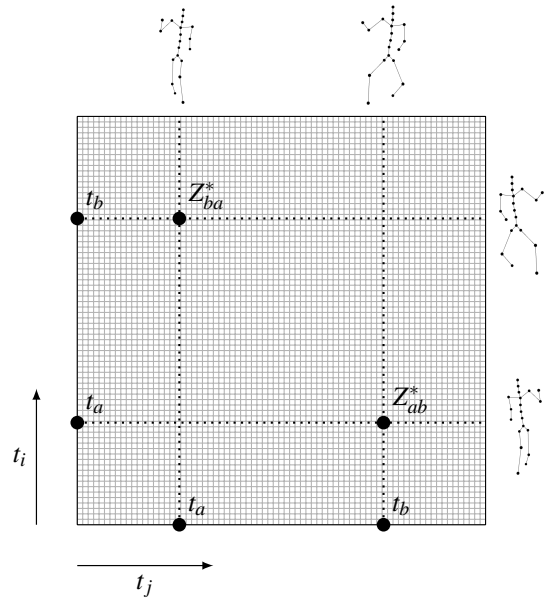

Figure 10: Representation of a Z^*_{ij} with many time points

Since D^*_{ij} is a pseudometric it lacks the indiscernability property of proper metrics.

$$D^*_{ii} \neq 0 \text{ for all i} \tag{22}$$

It follows that the diagonal elements of the anti-similarity matrix $Z*_{ij}$ are not necessarily equal to one. If it is the case that over some index the diagonal elements of the anti similarity matrix are one it means that the set of configuration states is symmetric.

$$Z^*_{ii} = 1 \longleftrightarrow \overrightarrow{\Psi}(t_i) = \overrightarrow{\Psi}^*(t_i) \tag{23}$$

Symmetric configuration states are associated with a proximity signal along the identity axis of the anti-similarity spectrum as shown in Figure 11.

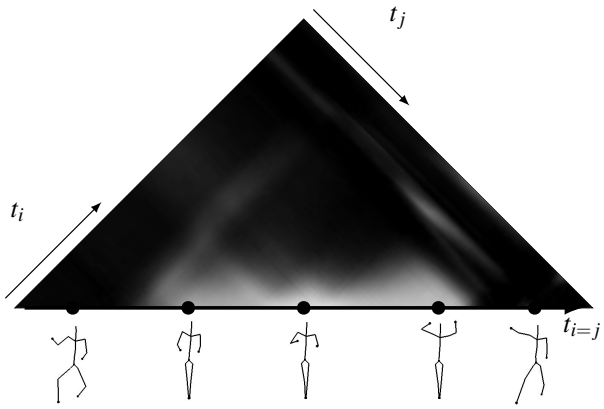

Figure 11: Z^*_{ij} plot of symmetric motion.

4.3 Bilateral Motion Spectra

In order to visualize Z_{ij} and Z^*ij simultaneously we use orthogonal color vectors, red and cyan, to plot Z_{ij} and Z^*ij respectively and overlap the two spectra. When the proximity signals of Z and Z^* overlap we get the addition of red and cyan to generate a greyscale signal. In the case that $Z_{ij} = 1$ and $Z^*_{ij} = 1$ we know that we have repetition and symmetry. This corresponds visually to a white proximity signal in the combined spectrum. This combined color plot is the bilateral motion spectrum (Z_{ij}, Z^*_{ij}). The addition of Z_{ij} and Z^*_{ij} is shown in Figure 12. The motion sequence is the same as that presented in Figure 11.

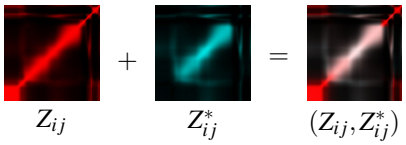

Figure 12: Overlay of Z and Z^* plots to generate the Z/Z^* plot or bilateral motion spectrum.

4.4 Reflected State Repetition

When a state of articulation repeats on the reflected side we observe a cyan proximity signal off the identity axis. This is shown in Figure 13. The red proximity signal on the identity axis indicates $\Psi(\overrightarrow{t_a t_b})$ does not pass through a symmetry state. The off axis proximity signal indicates a similarity between $\Psi(t_a)$ and $\Psi(t_b)$.

$$\forall\, i : \Psi(t_i) \neq \Psi^*(t_i) \tag{24}$$

$$\Psi(t_a) = \Psi^*(t_b) \tag{25}$$

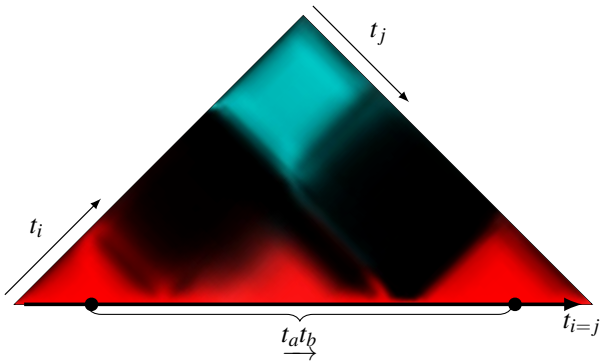

Figure 13: Bilateral motion spectrum with reflected state repetition.

4.5 Anti-Phase Motion

A movement sequence such as walking, which proceeds through a series of asymmetric configuration

states and then repeats on the other side, yields a particular motif in its bilateral motion spectrum. In other words, the complete motion cycle consists of a movement phrase which is performed and then the reflected version of that phrase is performed. This kind of movement is referred to as anti-phase motion because the left side of the body is 180 degrees out of phase with the right hand side of the body. The associated visual motif consists of parallel red and cyan proximity signals. This type of bilateral motion spectrum is shown in Figure 14. The red identity axis indicates all the states of $\Psi(\underrightarrow{t_a t_c})$ are asymmetric.

$$\forall\, i : \Psi(t_i) \neq \Psi^*(t_i) \tag{26}$$

The cyan horizontal off axis proximity signal, parallel to the identity axis, indicates reflected path repetition.

$$\Psi(\underrightarrow{t_a t_b}) = \Psi^*(\underrightarrow{t_b t_c}) \tag{27}$$

The red off axis proximity signal at the top of the triangle indicates the whole motion path $\Psi(\underrightarrow{t_a t_c})$ is cyclic.

$$\Psi(t_a) = \Psi(t_c) \tag{28}$$

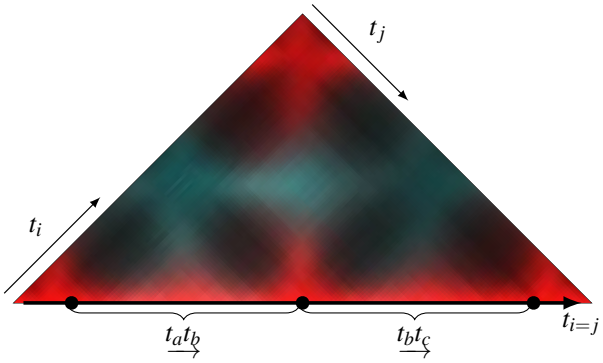

Figure 14: Bilateral motion spectrum of anti-phase motion.

4.6 Palindromic Anti-Phase Motion

A motion path which proceeds through a series of configuration states, reverses palindromically, and then repeats on the other side has a distinct bilateral motion spectrum. In other words the complete motion cycle consists of a movement phrase which is executed and then the reflected version of that phrase is performed reversed in time. We term this type of motion palindromic anti-phase. This type of motion passes through a symmetric state. Figure 15 presents the bilateral motion spectrum of a palindromic anti-phase motion sequence. The cyan proximity signal, extending perpendicular to the identity axis, indicates reflected path repetition reversed in time.

$$\Psi(\underrightarrow{t_a t_b}) = \Psi^*(\underleftarrow{t_b t_c}) \tag{29}$$

The white section of the identity axis indicates the motion path passes through a symmetry state at t_b.

$$\Psi(t_b) = \Psi^*(t_b) \tag{30}$$

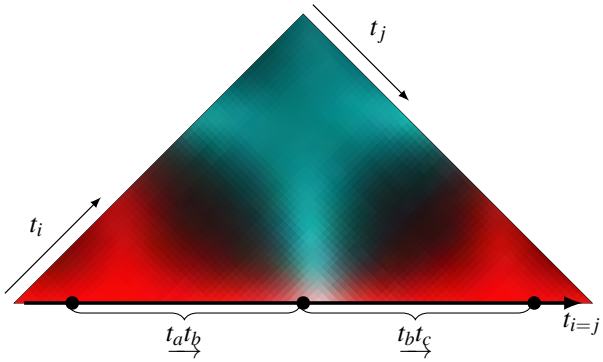

Figure 15: Bilateral motion spectrum of palindromic anti-phase motion.

4.7 Example Sequence

Figure 14 shows the bilateral motion spectrum for a sequence of motion phrases. The movements are jumping jacks, jogging in place, deep knee bends, twisting, side bends, side reaching and side gesturing. Each motion phrase generates one of the characteristic motifs covered above. Each phrase is also distinct as it generates a minimal off-diagonal proximity signal.

5 APPLICATIONS

5.1 Medicine and Human Performance

This type of analysis could be effective in identifying pathological movement patterns in patients, athletes and performers. A subject could be asked to execute a series of movement sequences in a clinical setting which tested various types of spatio-temporal pattern capacities. Motion capture data could be recorded, processed and analyzed to identify any motion asymmetries or other pathologies.

5.2 Gaming and Human Computer Interaction

This type of analysis could be performed by a gaming system in real time in order to recognize patterned motion such as dancing. Rhythm and motion patterns could be recognized and integrated into the game play.

5.3 Biological and Anthropological Applications

This type of analysis could provide a taxonomy of human and animal movement for the effective databasing of various motions. For example a database of dance would benefit from such a structural taxonomy.

6 FUTURE WORK

In the future we hope to record longer movement sequences. Choreographed movements such as ballet dances, Ashtanga yoga series or martial arts forms should have high degrees of spatial and temporal symmetry. Bilateral motion spectra of such sequences would be able to represent the patterns within such choreographed movement sequences.

It could also be fruitful to apply this analysis for subspaces of the configuration space of the body, looking at the spine, legs and arms separately.

7 CONCLUSION

In this paper, we presented a novel data structure for analyzing, characterizing and representing continuous human motion data. The data structure was able to effectively identify spatial and temporal movement patterns. Our main contributions are summarized below.

1. We formalized existing methods of motion capture analysis using metric and metric space theory.
2. We functionalized existing methods of motion capture analysis in order to characterize temporal features of human movement including stillness, rapidity, state repetition, path repetition and palindromic repetition.
3. We enhanced existing methods of motion capture analysis in order to characterize spatial movement patterns including symmetric motion, anti-phase motion and palindromic anti-phase motion.
4. We developed a concise visual representation of human motion which can express a wide variety of spatial and temporal pattern motifs.

REFERENCES

Alankus, G. (2005). Animating character navigation using motion graphs. Master's thesis, Middle East Technical University.

Arikan, O. and Forsyth, D. A. (2002). Interactive motion generation from examples. In *Proceedings of the 29th Annual Conference on Computer Graphics and Interactive Techniques*, SIGGRAPH '02, pages 483–490. ACM.

Huynh, D. (2009). Metrics for 3d rotations: Comparison and analysis. *Journal of Mathematical Imaging and Vision*, 35:155–164.

Kovar, L., Gleicher, M., and Pighin, F. (2002). Motion graphs. In *Proceedings of the 29th Annual Conference on Computer Graphics and Interactive Techniques*, SIGGRAPH '02, pages 473–482. ACM, ACM.

Murray, M., Li, Z., and Sastry., S. S. (1994). *A Mathematical Introduction to Robotic Manipulation*. CRC Press.

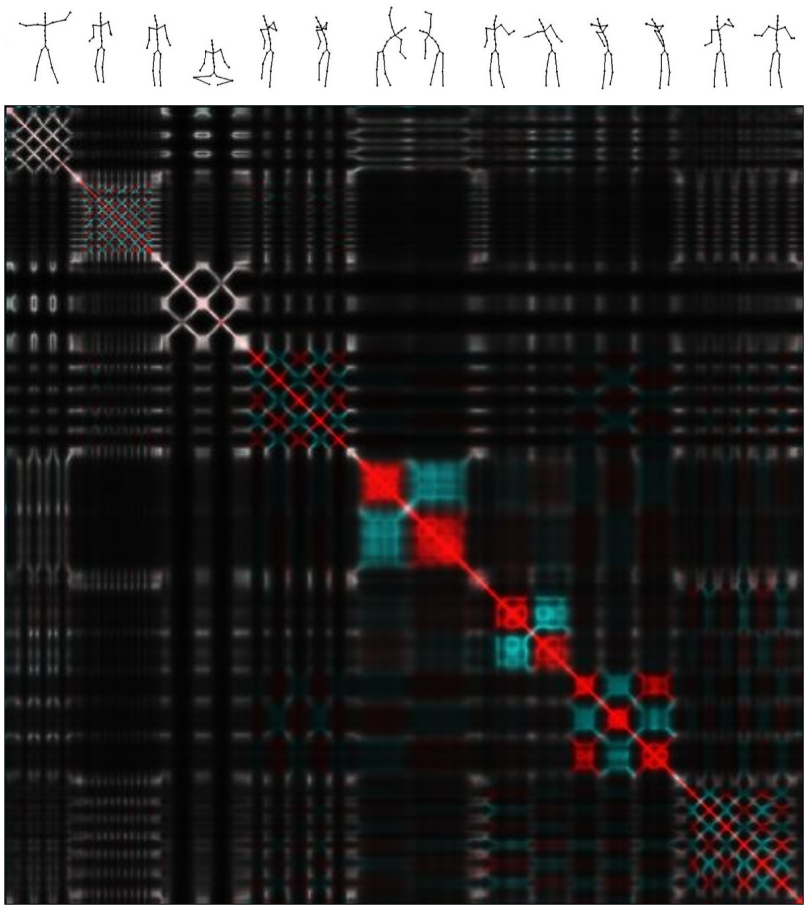

(Z_{ij}, Z^*_{ij})

Figure 16: Bilateral motion spectrum of various movement phrases.